Morphology of oriented calcium alginate gels obtained by the flow-gelation method

Fumiyoshi Yokoyama, E. Chukwura Achife, Masaki Matsuoka, Kaoru Shimamura, Yuhiko Yamashita and Kazuo Monobe

Department of Applied Chemistry, Faculty of Engineering, Okayama University, Tsushima, Okayama 700, Japan

(Received 7 August 1990; revised 26 September 1990; accepted 12 October 1990)

Cylinder-shaped oriented gels of calcium alginate were prepared by extruding a 2.6 wt% aqueous solution of sodium alginate (guluronate rich) into $CaCl_2$ solution through a glass tube. Effects of flow rates on chain orientation in solution and in the gel were examined by polarized optical microscopy. During flow, chains underwent planar orientation along the tube wall, which was reflected in the gel state. Increasing the flow rate increased the coil–stretch transition in solution but led to disorientation of chains in the gel due to increasing die swell and longitudinal shrinkage. This effect resulted in the occurrence of the highest anisotropy of the gel at low flow rate. Chain orientation in the gel was characterized by tilting towards the tangential direction with the appearance of a small negative birefringence, which was transformed to a large positive birefringence on drying due to chain realignment in the longitudinal direction. The morphology of the gel was deduced to be sheet-like structures stacked cylindrically with strong intrasheet binding. Scanning electron microscopy and wide-angle X-ray diffraction were both used in the investigation.

(Keywords: calcium alginate; flow; gelation; birefringence; morphology)

INTRODUCTION

Alginate is a naturally occurring polysaccharide which is usually obtained from brown algae. It is a copolymer composed of β-D-mannuronate (M) and α-L-guluronate (G) residues, both of which are 1,4-linked. The residues are arranged either as homopolymeric blocks (MM or GG) or as alternating blocks (MG). From light scattering studies, viscosity measurements[1–3] and conformational analyses[4] it has been argued that the extension of the three types of blocks increased in the order: MG < MM < GG.

It is well known that gelation readily occurs when an aqueous solution of sodium alginate comes into contact with metallic divalent cations such as calcium, lead, zinc, etc., either directly or via a semipermeable membrane. Stronger binding of the metal ions occurs with G blocks than with M blocks. Changes in chain conformation on gelation have been studied previously using circular dichroism and the optical rotary dispersion method[5–8], indicating the occurrence of a more extended chain conformation in the gel state than in free solution. The 'egg box' model[5] for metallic polyguluronate gels, where the interchain cavities provide suitable sites for coordination of metal ions, was then proposed. Until now, this has been accepted as the basic structural model.

Fibrous gels are readily formed by extrusion of dilute or semidilute sodium alginate solutions through tubes into the gelation medium containing divalent metallic ions. The X-ray diffraction patterns of the dried gels from elongated fibrous gels have been known to exhibit fairly good fibre orientation. Therefore, X-ray crystallography has been performed on dried fibres of metallic and acidified forms of alginate[9–13]. However, little has been published on the morphology of the as-formed wet gels[14].

Recently, we showed that agarose or agar, a polysaccharide with a high gelling ability, gave optically anisotropic gel textures when the aqueous solutions gelled during flow[15]. The high chain orientability of agarose under flow was considered to be due to the inherent rigidity of the helical chains. A number of polymers have been reported whose solutions exhibit optical anisotropy only during flow[16,17]. It is an interesting feature of gel-forming polymers that anisotropic structures attained during flow are more or less retained in the gel state, even after the release from the flow field. In the present study, calcium alginate gels were prepared by the flow-gelation method, in which a semidilute solution of sodium alginate was extruded through a small tube into $CaCl_2$ solution under various flow rates. The sodium alginate used here is rich in guluronate content. This paper studies chain orientation during flow in the tube; the influence of gelation on chain orientation in as-formed gels; the textural morphology of the gels; and chain orientation in dried gels. Polarized optical microscopy, together with scanning electron microscopy and wide-angle X-ray diffraction were used in the studies.

EXPERIMENTAL

Sample preparation

G-rich sodium alginate of commercial reagent grade (Ishizu Pharmaceutical Company, Japan) was used. This was dissolved in deionized and distilled water to obtain a 2.6 wt% solution, which was stored for 1 day to ensure complete dissolution. Cylinder-shaped gels were prepared by extruding the solution through a glass tube (2 mm diameter, 150 mm long) fitted to a syringe (16 mm diameter) into 0.5 mol l^{-1} $CaCl_2$ solution under various flow rates ranging from 8 to 950 mm s^{-1}. The flow rates were achieved using a motor-driven device [shear rates at the wall were 32–3800 s^{-1}, if the relation[18] $4Q/\pi R^3$

0032-3861/91/162911 06

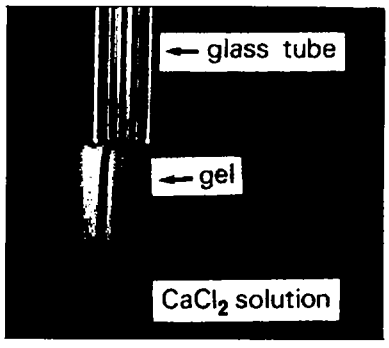

Figure 1 Diametric expansion of gel formed on extrusion of sodium alginate solution into $CaCl_2$ solution at 570 mm s^{-1}. The inner and outer diameters of the tube are 2 and 4 mm, respectively

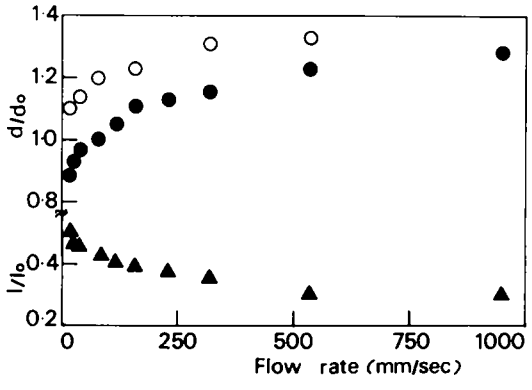

Figure 2 Diametric expansion (circles) and longitudinal shrinkage (triangles) ratios of extrudates in $CaCl_2$ solution as a function of flow rate in the tube. The open and closed symbols represent the values immediately after and 1 day after extrusion, respectively; the diameter d_0 is 2 mm and the length l_0 is defined as the length derived by dividing an extruded volume by the cross-sectional area of the tube; d and l refer to extrudates

was used, where Q and R are volumetric flow rate ($mm^3\ s^{-1}$) and radius of the tube (mm), respectively]. The immediate flow into the gelation medium was also photographed. The gels thus obtained were left in the $CaCl_2$ solution for 1 day. 'Washed'-gel samples were also obtained by soaking the as-formed gels in occasionally exchanged water. (The washing was carried out in order to remove free and weakly bound calcium ions.) Some of the 'washed' gels were gradually dried for 1 week at room temperature by suspending them ($\sim 30\ cm^2$) with both ends fixed in order to prevent longitudinal shrinkage and others were rapidly dried under vacuum. Alginic acid fibres were obtained by acidification of the former dry gels in an aqueous solution of 0.5 mol l^{-1} HCl for 1 h, followed by soaking in water for 2 h and drying at room conditions for 2 days. The transverse and longitudinal cut sections of the wet gels were also prepared (thickness < 1 mm); particular attention was paid in the cutting of the latter in order to obtain a symmetric shape.

Measurements

The gels obtained were examined using a Nikon polarized optical microscope, under crossed-polarizers with white light; a sensitive tint plate with retardation (530 μm) and a Berek rotary compensator[19] were used to obtain the optical anisotropy and estimate the birefringence values, respectively. The birefringence measurements for wet gels were carried out in $CaCl_2$ solution or in water and those for the gradually dried gels were performed in benzyl alcohol in order to eliminate both light reflections and form birefringences[20].

For the alginate solutions under flow in the tube and the resultant cylindrical gels, the intensities of the light transmitted normal to the cylinder axis were measured at 45° on the polarized microscope stage; the intensities were normalized with that transmitted from the tint plate.

The rapidly dried gels were fractured at liquid nitrogen temperature. The fractured surfaces were decolated with evaporated gold and studied using a scanning electron microscope (Hitachi S-405).

Changes in retardation with drying time were examined using the method in which both ends of a few centimetres of 'washed' gels were fixed on a slide glass with tape and allowed to dry freely on the polarized microscope stage at room temperature.

The wide-angle X-ray diffraction patterns of the gradually dried fibres of calcium alginate and of the corresponding acidified fibres were taken using graphite-monochromated Cu Kα radiation.

RESULTS AND DISCUSSION

Extrusion into the gelation medium

Extrusion (at a flow rate of 570 mm s^{-1}) into a $CaCl_2$ solution is shown in *Figure 1*, where die swell[21] is observed and the surface of the extrudate is opaque (evidence of complexation). As shown in *Figure 2*, by increasing the flow rate, the die swell and the related longitudinal shrinkage increased, showing a large flow rate dependency in the lower flow rate range. At any flow rate, the former was greatest immediately after extrusion into the gelation medium. We confirmed that die swell was absent on extrusion in air. Consequently, this phenomenon seems to be related to the rubber-like nature of the gel network formed on extrusion. The extrusion thus should alter the chain orientation which was attained during flow in a tube, i.e. a tilting or a disorientation of chains over the whole gel phase. Application of a flow rate of 950 mm s^{-1} resulted in a notable curl of the gel.

Transmitted light intensities of the solutions and gels

In the present sodium alginate solution under flow, the intensity of the light transmitted normal to the cylinder axis increased with increasing flow rate, as shown in *Figure 3*. This is attributed to the increase in the number of coil–stretch transitions, as is often the case for forced flow in polymer solutions[16,17]. By the use of a sensitive tint plate, it was confirmed that with increasing flow rate the observed retardation increased positively along the wall surface. However, even at the highest flow rate, the retardation integrated along the diameter was too small to determine whether it was positive or negative. These results indicate that the alginate chains under flow have a strong tendency to undergo planar orientation along the tube wall rather than uniaxial orientation along the flow direction.

The light intensities from the as-formed cylindrical gels are also given in *Figure 3*. The intensity of the gel obtained by extrusion under the lowest flow rate (8 mm s^{-1}) is significantly higher than that from the corresponding flowing solution. This is due to a complexation effect: chains are transformed into a more

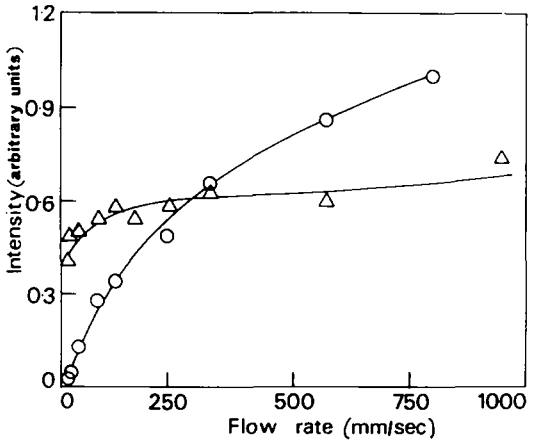

Figure 3 Transmitted light intensities of sodium alginate solution under flow (○) and calcium alginate gel fibre (△) as a function of flow rate in the tube. The intensities are normalized by that of the sensitive tint plate (530 μm)

Figure 4 Typical features of a polarized optical micrograph of a cylinder-shaped calcium alginate gel fibre. The arrow indicates the total flow direction

extended chain conformation on gelation[5-8], i.e. the resultant rod-like complexed bundles of chains are assumed to exhibit a high orientability along the gel surface. On the other hand, the low degree of flow rate dependency of intensity is recognized with increasing flow rate. The origin for this is mainly ascribed to the large deformation on gelation mentioned above through which chain orientation attained during flow in the tube is distorted.

General features of optical anisotropy in wet gels

There were some features commonly recognized in the polarized optical microscopic observations of the as-formed gels. The alginate gel specimens, when viewed normal to the cylinder axis, exhibited nearly overall extinction at four positions 90° apart; the greatest light transmittance was attained at 45°. As shown in *Figure 4*, banded structures consisting of two extinction lines parallel to the cylinder axis were observed. The birefringences of the two outer bright regions were found to be positive, while that of the inner bright region between the extinction lines was noted to be negative; the latter birefringence corresponds to $\langle \Delta n_{zy} \rangle$ (as given later), a mean value of birefringence integrated along the diameter. The sign of the birefringence here refers to the cylinder axis. These features are independent of the extrusion rates.

In the transverse cut section of the above gel, a distinct

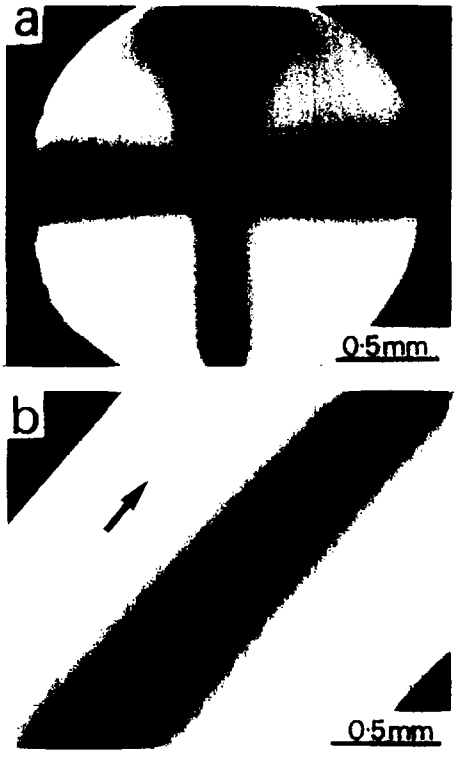

Figure 5 Typical features of polarized optical micrographs of (a) transverse and (b) longitudinal cross-sections of calcium alginate gel fibre. The arrow in (b) indicates the total flow direction

crossed extinction pattern was observed along the crossed polarizers, as shown in *Figure 5a*. This shows that the specimen is cylindrically symmetric. It thus allows the definition of refractive indices, n_x and n_y which are parallel to the radial and circumferential directions, respectively. The longitudinal cut section (*Figure 5b*) has an extinction pattern similar to the cylindrical gel in *Figure 4*. The refractive index, n_z can be defined parallel to the cylinder axis, as the overall extinction occurred at 0° and multiples of 90°. By observing these cut sections using the sensitive tint plate, it was found that $n_y > n_x$ and $n_z > n_x$. The optical anisotropy at a radial point in a gel specimen can be given by the three refractive indices, as indicated in *Figure 6*. An ellipsoid was assumed to be constructed.

In *Figure 7*, the observed birefringences, $\Delta n_{yx} = n_y - n_x$ for the transverse cut sections and $\Delta n_{zx} \approx n_z - n_x$ for the longitudinal* cut sections of the wet gels before and after soaking in water are plotted against r/r_0, where r_0 is the radius of the cut section and r is the radial distance from the centre. This is the case for a flow rate at 19.5 mm s^{-1} in the tube. Irrespective of whether the gels are 'washed' or 'unwashed', there are tendencies that: both Δn_{yx} and Δn_{zx} increase with r; and Δn_{yx} is slightly larger than Δn_{zx}. The order of refractive indices is then: $n_y > n_z \gg n_x$. We note here that the above tendencies shown in *Figure 7* were exhibited for all the gels obtained under various flow rates.

One of the origins of the radial-distance dependence of the birefringences, as presented in *Figure 7*, may be

* In the longitudinal cut section, the observed birefringences Δn_{zx} are approximate values of the true $n_z - n_x$, because, along the thickness, y-axis orientations are variable with respect to the incident light. However, we assumed that the relation, $n_z - n_x < n_y - n_x$ or $n_z < n_y$ might be true for any r, as the mean value of $n_z - n_y$ was negative

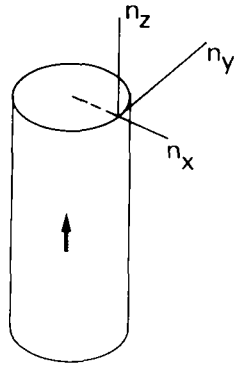

Figure 6 Co-ordinate system of refractive indices n_x, n_y and n_z relating to the cylinder-shaped gel fibre of calcium alginate. The arrow indicates the total flow direction

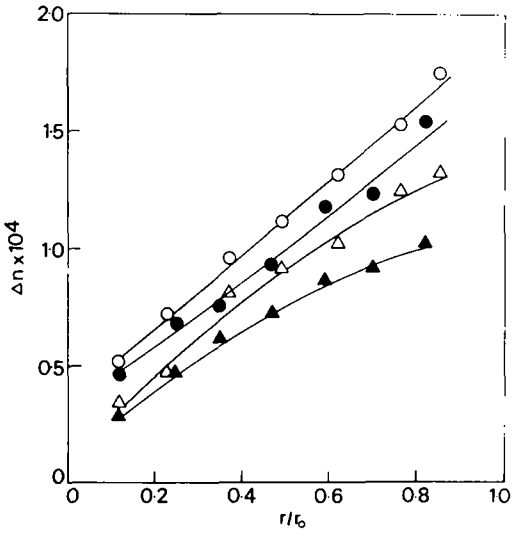

Figure 7 Birefringences of transverse (circles, $\Delta n \equiv \Delta n_{yx}$) and longitudinal (triangles, $\Delta n \equiv \Delta n_{zx}$) cut sections of gel fibre obtained at an extrusion rate of 19.5 mm s^{-1} as a function of r/r_0. The closed and open symbols represent the 'unwashed' and 'washed' specimens, respectively

attributed to the orientational and conformational relaxations of the chains. These are expected to have increased with distance from the gel surface, as a time lag for the penetration of calcium ions along the radius exists; the relaxations should cease after completion of the complexation. Another origin may be due to the elongation effect of shear stress which depends on radial distance.

The relation $n_y > n_z \gg n_x$ indicates that the orientational distribution of chains is greatest along the $y-z$ plane, reflecting that in the flowing solution. Small negative values of $\langle \Delta n_{zy} \rangle$, as given in *Figure 8*, seem to show that the mean chain orientation is directed towards the y-axis rather than the z-axis. The increase in the birefringences on soaking in water is found from *Figure 7*. Under the assumption that this effect originates from the reduction in n_x, it is suggesed that bindings of gel textures with calcium ions would be weak along the radial direction.

It should be noted that the oriented agarose hydrogel prepared by our method[15] in which a hot aqueous solution of agarose was gelled during flow in a tube showed a contrasting strong longitudinal orientation of chains. This difference lies in the fact that the deformation of texture during gelation was essentially avoided for this case.

Scanning electron microscopy of rapidly dried gels

Scanning electron micrographs of the xerogels dried under vacuum are shown in *Figure 9*. The specimens were soaked in water for 1 min (*Figure 9a*) and 2 h (*Figure 9b*). The xerogel morphologies were assumed to reflect those before drying, as it was considered that the rapid removal of water under vacuum did not allow sufficient time for large changes. However, certain degrees of deformation and aggregation of the textures during drying were not totally avoided. It was considered that cylindrically

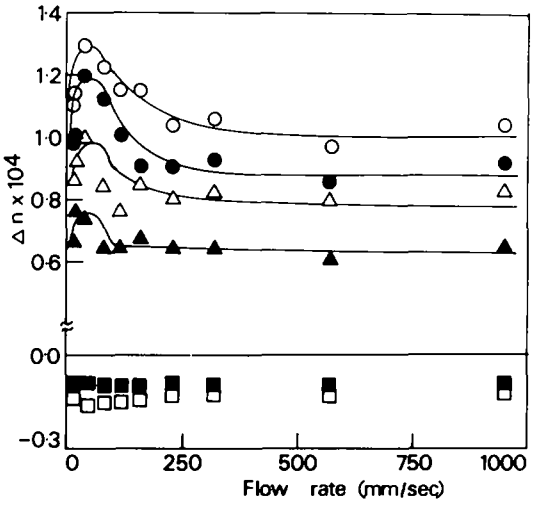

Figure 8 Birefringences (at $r/r_0 = 0.5$) of transverse (circles, $\Delta n \equiv \Delta n_{yx}$) and longitudinal (triangles, $\Delta n \equiv \Delta n_{zx}$) cut sections and as-formed cylinders (squares, $\Delta n \equiv \langle \Delta n_{zy} \rangle$) of wet gels, as a function of flow rate in the tube. The closed and open symbols represent 'unwashed' and 'washed' specimens, respectively

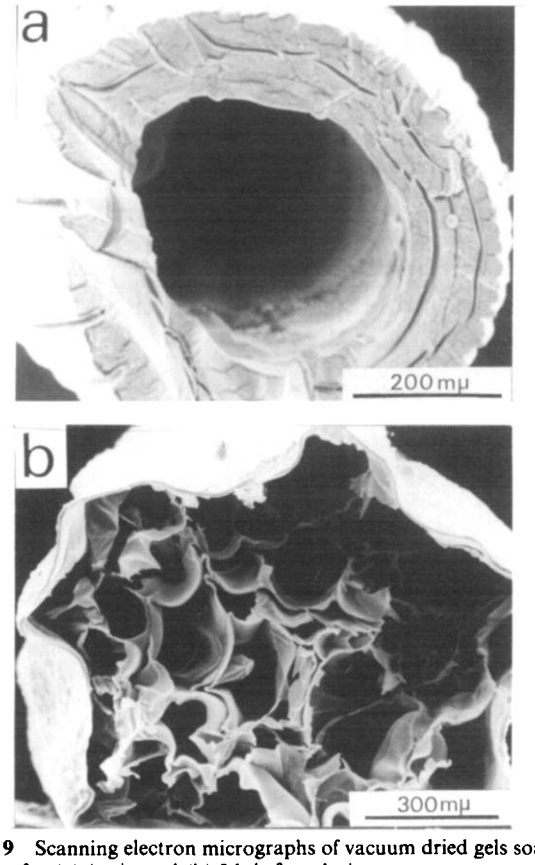

Figure 9 Scanning electron micrographs of vacuum dried gels soaked in water for (a) 1 min and (b) 2 h before drying

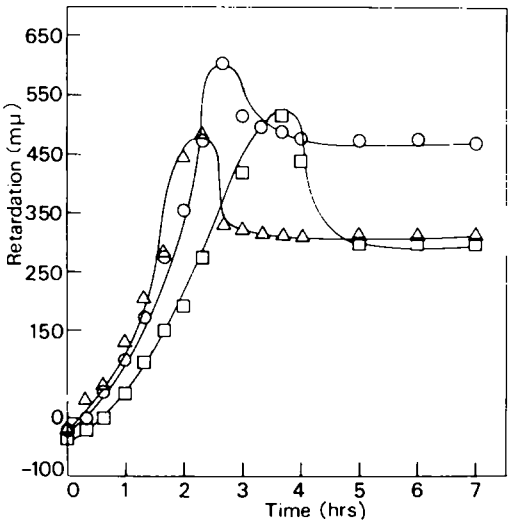

Figure 10 Retardations of gel fibres obtained at various extrusion rates as a function of drying time: (△) 8; (○) 32; (□) 160 mm s^{-1}

developed sheet structures tightly bound together (*Figure 9a*) but were separated from one another (*Figure 9b*). The outermost sheet in *Figure 9b* may correspond to a semipermeable membrane formed immediately after extrusion, through which exchange of metal ions is assumed to have occurred, with the later formation of the inner membranes. This time-dependent structural formation may be a cause of the reduced anisotropy of the inner texture (*Figure 7*).

The morphologies in *Figure 9* suggest that intrasheet bindings of calcium ions and hydrogen bonds are strong, while intersheet ones are weak. From a crystallographic point of view, it is conceivable that the sheet surface corresponds to an equatorial plane of polyguluronate crystals[13,14], along which chains interact strongly. The morphologies of the rapidly dried gels did not show any dependence on the flow rates applied.

Flow rate dependency of optical anisotropy in wet gels

In *Figure 8*, Δn_{yx} and Δn_{zx} for the cut sections are plotted as a function of the flow rate, together with $\langle \Delta n_{zy} \rangle$ for the cylindrical gels; Δn_{yx} and Δn_{zx} are represented by the values at $r/r_0 = 0.5$. With increasing flow rate, both Δn_{yx} and Δn_{zx} increase towards the respective maximum. In this narrow flow rate range, as expected from *Figure 3*, the chain orientation attained during flow is enhanced through complexation. Consequently, with increasing flow rate, complexed bundles with higher chain orientation result along the gel surface. In each cut section, a transition from the maximum to the lower plateau is observed with increase in flow rate. This is the result of a counterbalance between two conflicting effects of flow rate: one is the increasing orientation of chains in solution and the other is the increasing disorientation of chains during gelation.

As already pointed out, $\Delta n_{yx} > \Delta n_{zx}$ and the increments in the birefringences of 'washed' gels are seen over the entire flow rate range. The differences in $\langle \Delta n_{zy} \rangle$ between 'unwashed' and 'washed' gels are very small, indicating a minor change in chain orientation within the $y-z$ plane.

Change in retardation during drying

The 'washed' gels were of constant length on the stage of the polarized optical microscope and were dried at room conditions. The first change in the birefringence pattern on drying was the disappearance of the extinction lines. Then, the retardation changed from negative to positive and greatly increased towards the maximum, followed by a lower plateau, as found for various flow rates (*Figure 10*). We assumed that this phenomenon was due to the change in chain orientation to uniaxial (z-axis) alignment during drying. In each case, the difference between the maximum and the plateau is attributed to the form birefringence[20] which emerged strongly but temporarily when the macroscopically uniaxial-oriented chains were surrounded by a comparable volume of water having a lower refractive index. Similar retardation–time curves were obtained for other specimens.

Flow rate dependency of optical anisotropy of xerogels obtained under room conditions

In *Figure 11*, the birefringences for the xerogels obtained by suspending samples with both ends fixed at room conditions are plotted against the flow rate in the tube; the birefringences are positive. The shape of the curve is similar to that of the cut sections in *Figure 8*. These results are attributed to the change in chain orientation during drying. In the scanning electron microscopic examination of the xerogels, the sheet-like structures were not observed, probably due to adhesion of the textures. The influence of the die swell and the longitudinal shrinkage during gelation is reflected in the diameter increase in the xerogels.

X-ray diffraction patterns

The wide angle X-ray diffraction patterns of calcium alginate xerogel and the corresponding acidified fibre are given in *Figure 12*. The former was from a flow rate of 9.5 mm s^{-1} and with the highest birefringence (*Figure 11*). The patterns are those of fibre orientation[9,13]. The pattern of the acidified fibre is clearer than that of the calcium alginate fibre, showing the strongest (101) reflections of the polyguluronic acid crystals (the fibre axis is the b-axis). The diffuseness of the pattern for the calcium alginate fibre, particularly along the equatorial direction results from the existence of disorder in the lateral chain packing in the solid phase. This suggest that the calcium-complexed chains are very rigid, like liquid crystalline polymers. There was no large observed difference in the fibre pattern of another specimen with the lowest birefringence (*Figure 11*).

CONCLUSIONS

A semidilute sodium alginate solution was extruded from a small glass tube into a $CaCl_2$ solution with various

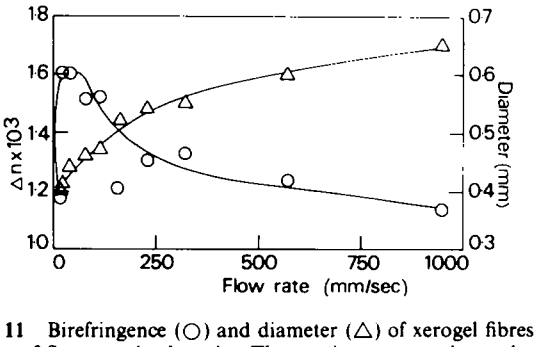

Figure 11 Birefringence (○) and diameter (△) of xerogel fibres as a function of flow rate in the tube. The specimens were those obtained by drying the 'washed' gels of constant length at room conditions

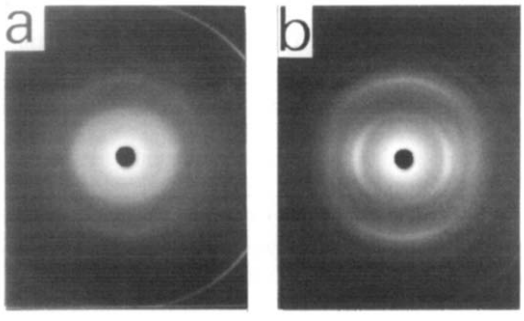

Figure 12 Wide-angle X-ray diffraction patterns of (a) calcium alginate xerogel fibre (flow rate 9.5 mm s^{-1}) and (b) the corresponding acidified fibre

flow rates to obtain oriented gels. We were able to obtain some basic data from this gelation system:

1. Sodium alginate solution under flow seemed to show a planar orientation along the tube wall, accompanied by an increasing number of coil–stretch transitions with flow rate. This planar orientation was reflected in the gel state.
2. The high anisotropy forming ability of the gel lay in the formation of rigid complexed bundles of chains which are much more extended than in solution under flow.
3. The flow rate had two conflicting effects on chain orientation: one was the shear flow effect found in solution; the other appeared through increasing die swell and longitudinal shrinkage during gelation. This led to disorientation of chains. Due to the counterbalance of the two effects, the highest anisotropy of the gel was accomplished in a low flow rate range.
4. The large deformation during gelation appeared to result in orientation of chains towards the *y*-axis. This was related to the negative birefringence observed along the diameter.
5. The morphology of the wet gels was assumed to be characteristic of sheet-like structures stacked cylindrically; there were strong intrasheet bindings and weak intersheet bindings.
6. The xerogels obtained by drying the wet gels of constant length at room conditions showed fibre orientation with positive birefringences. This was due to the orientational change to uniaxial alignment during drying. The flow rate at which the highest chain orientation was attained in the xerogels was in the same range as for the wet gels.

This study is the first to describe chain orientation and structural anisotropy by the flow-gelation method. The effects of metal ions and hydrogen bond on birefringences are not yet completely established, so our interpretations may be modified by further studies.

REFERENCES

1 Harkness, M. L. R. and Wassermann, A. *J. Chem. Soc.* 1952, 497
2 Smidsrød, O. *Carbohydrate Res.* 1970, **13**, 359
3 Smidsrød, O. *Carbohydrate Res.* 1973, **27**, 107: *Faraday Discuss. Chem. Soc.* 1974, **57**, 263
4 Whittington, S. G. *Biopolymers* 1971, **10**, 1481, 1617
5 Grant, G. T., Morris, E. R., Rees, D. A., Smith, P. J. C. and Thom, D. *FEBS Lett.* 1973, **32**, 195
6 Morris, E. R., Rees, D. A. and Thom, D. *Carbohydrate Res.* 1978, **66**, 145
7 Thom, D., Grant, G. T., Morris, E. R. and Rees, D. A. *Carbohydrate Res.* 1982, **100**, 29
8 Morris, E. R., Rees, D. A. and Young, G. *Carbohydrate Res.* 1982, **108**, 181
9 Mackie, W., Perez, S., Rizzo, R., Taravel, F. and Vignon, M. *Int. J. Biol. Macromol.* 1983, **5**, 329
10 Atkins, E. D. T., Mackie, W. and Smolko, E. E. *Nature* 1970, **225**, 626
11 Mackie, W., Parker, K. D. and Smolko, E. E. *Polym. Lett.* 1971, **9**, 311
12 Atkins, E. D. T. and Nieduszynski, I. A. *Biopolymers* 1973, **12**, 1865
13 Atkins, E. D. T. and Nieduszynski, I. A. *Biopolymers* 1973, **12**, 1879
14 Sterling, C. *Biochem. Biophys. Acta* 1957, **26**, 186
15 Yokoyama, F., Momoda, J., Maki, H., Shimamura, K. and Monobe, K. in 'Cellulose. Structural and Functional Aspects' (Eds. J. F. Kennedy, G. O. Phillips and P. A. Williams), Ellis Horwood, New York, 1989, p. 311
16 Miles, M. J., Tanaka, K. and Keller, A. *Polymer* 1983, **24**, 1081; Keller, A. and Odell, J. A. *Coll. Polym. Sci.* 1985, **263**, 181
17 Peifer, D. G., Kim, M. W. and Lundberg, R. D. *Polymer* 1985, **27**, 493
18 Brysden, J. A. 'Flow Properties of Polymer Melts', Illife, London, 1970, p. 24
19 Sawyer, L. C. and Grubb, D. T. 'Polymer Microscopy', Chapmann and Hall, New York, 1987
20 Slayter, E. M. 'Optical Methods in Biology', Wiley Interscience, New York, 1970, p. 336
21 Lodge, A. S. 'Elastic Liquids', Academic Press, London, 1964, p. 242